Erosion Modeling over a Steep Slope: Application to a Dike Overtopping Test Case

Sylvie Van Emelen,
PhD student, Fond de la Recherche Scientifique – FNRS & Inst. of Mechanics, Materials and Civil Eng., Université catholique de Louvain, Louvain-la-Neuve, Belgium. Email: sylvie.vanemelen@uclouvain.be

ABSTRACT: The most violent floods are due to the failure of embankments, such as dams or levees. In case of dike overtopping, the erosion over the steep downstream slope is one of the main processes leading to the breaching. This study analyses the ability of numerical models to simulate this process. Various sediment transport formulations are presented and compared. A special attention is paid to the ways to account for the slope effects in these expressions. These sediment transport equations are included in two different one dimensional numerical models, based on the assumptions of a clear water layer and of a sediment-water mixture layer respectively. These two models are applied on a new dike overtopping experimental test-case, representing a small-scale sand dike with a sand layer downstream of the dike. The numerical results are compared to the experimental measurements, with a special attention paid on the sediment transport formulation, on the steep slope correction factor, and on the choice of the numerical model.

KEY WORDS: Breaching, Numerical simulation, Sediment, Erosion, Experiment

1 INTRODUCTION

Failure of embankments create fast transient flows, potentially generating critical material and human damages. In the particular case of earthen embankments, the main cause of failure is the breaching due to overtopping flows. This breaching process is driven by intense erosion of the downstream slope of the dike. This intense erosion process occurring over a steep slope needs to be accurately understood in order to improve our ability to model these flood events.

The bed slope has a predominant impact on sediment transport in various situations. So, various studies have focused on the particular impact of bed slopes on sediment transport, in a wide range of situations. These include mountain stream floods and resulting debris flows, overland run-off, landslide, and dike breaching modeling. All these flows are characterized by various sediment ranges, flow discharges and water depths, so results for a particular domain are usually not appropriate for other ones.

Several sediment transport equations have been proposed in the literature. These equations are generally empirically developed under the assumption of steady flow. Moreover they usually do not account for steep bed slopes and high shear stresses. Regarding the high transport intensity, El Kadi Abderrezzak and Paquier (2011) compared several sediment transport equations for dam-break tests on horizontal bed. Regarding the influence of steep slopes, Fernandez-Luque and van Beek (1976) proposed a correction for the critical shear stress in case of a streamwise slope, while Wu and Wang (2008) included the effect of the slope through a modified tractive force.

All these equations can be coupled to a physically-based numerical model to simulate the erosion process. One-dimensional numerical models of flow over erodible beds can be classified in four groups

depending on the interaction between water and sediment: Clear Water Layer models (CWL), Mixture Layer models (ML), Two-Phases models (2P), and Two-Layer models (2L). While CWL models represent one layer of clear water flowing over a movable sediment bed (e.g. Cunge and Perdreau 1973, Goutiere et al. 2008), ML models involve one layer composed of a mixture of sediment and water, characterized by a variable density, over an erodible bed (e.g. Capart and Young 1998, Cao et al 2004, Wu and Wang 2008). Models such as 2P and 2L models are more complex, the first one representing the flow as one layer of water-sediment mixture but with different momentum equations for water and sediment (Greco et al., 2009), and the second one representing a layer of clear water over a layer of water-sediment mixture on a movable bed (e.g. Fraccarollo et al. 2003, Zech et al. 2008). In this study only CWL and ML models will be used.

Within this framework, this paper analyses the ability of ML and CWL models to simulate bed-load transport on steep slopes with high shear stresses. Both types of models will be compared with an experimental test case conducted at the Hydraulics Laboratory of the Université catholique de Louvain, Belgium. This test case presents the particularity to study both the dike erosion and the bed evolution downstream of the dike.

The paper is organized as follows. First, various sediment transport formulations are described and compared. Then, the impact of a steep slope on the sediment transport modeling is highlighted. Secondly the CWL and ML numerical models are described. Then the experimental dike overtopping test case is briefly described. Finally, the numerical results are compared to the experimental measurements, with a special attention to the impact of the sediment transport formulation, to the steep slope correction factor, and to the choice of the numerical model.

2 SEDIMENT TRANSPORT RATE

2.1 Various sediment transport formulations

During dike overtopping, sediment is transported downhill due to intense bed-load induced by the steep slope gravity component and by the high shear stresses acting on the bed. Several empirical expressions were developed to formulate the sediment transport capacity. All these formulations were empirically calibrated. A selection of these formulations and their conditions of calibration are reported in Table 1.

Table 1 Selected bed-load sediment transport formulations

References	Non-dimensional bed-load formulation	Calibration conditions		
		d (mm)	S_0	τ_*
Meyer-Peter & Müller (1948)	$q_{*s,MPM} = 8(\tau_* - \tau_{*c})^{3/2}$	0.4-29	<0.02	<0.25
Wong and Parker (2006)	$q_{*s,WP} = 3.97(\tau_* - \tau_{*c})^{3/2}$	0.4-29	<0.02	<0.25
Smart & Jäggi (1983)	$q_{*s,S} = 4.2(u/u_*)S_f^{0.6}\tau_*^{0.5}(\tau_* - \tau_{*c}(\alpha_0))$	0.4-29	0.073-0.2	0.1-3.3
Abrahams (2003)	$q_{*s,A} = \tau_*^{1.5} u / u_*$	3-10.5	0.03-0.21	0.6-1.83
Camenen & Larson (2005)	$q_{*s,CL} = 12\tau_*^{1.5}\exp(-4.5\tau_{*c}/\tau_*)$	0.084-200	0.03-0.2	0.1-3.3
Wu *et al.* (2000)	$q_{*s,W} = 0.0053\cdot\left((n'/n)^{1.5}(\tau_*/\tau_{*c})-1\right)^{2.2}$	0.062-128	<0.016	-

Note: $q_{*s} = q_s(g(s\text{-}1)d^3)^{-0.5}$ is the non-dimensional sediment transport with d the sediment diameter, $s = \rho_s/\rho_w$ the ratio of sediment and water densities and g the gravity. $\tau_* = hS_f/((s\text{-}1)d)$ is the non-dimensional bed shear-stress (Shields number) and τ_{*c} its critical value (0.047 for MPM, 0.0495 for WP, 0.03 for W). τ_{*c} (α_0) is defined in Eq. (1). n is the global Manning coefficient for the bed and n' is the Manning's coefficient corresponding to grain roughness ($n = n$' here). S_0 is the bottom slope and $S_f = \tan(\alpha_f)$ is the friction slope. h is the water depth, q the discharge per unit width, u the velocity, and u_* is the shear velocity

Figure 1 shows the comparison between the different formulations of Table 1 for uniform flows ($S = S_0 = S_f$) on various bed slopes S_0. The following parameters are chosen: sediment diameter d = 2 mm, Manning coefficient $n = d^{1/6}/21.1 = 0.0168$ s m$^{-1/3}$ following Strickler's (1923) formula, flow discharge

per unit width q = 40 l/s/m. The water depth $h_u = (qn/S^{0.5})^{1.5}$, the velocity, and the Shields parameter depend on the bed slope for uniform flows. We observe in Fig. 1 that the largest effect of the slope on the transport rate q_s arises from the shear stress formulation in Wu's and Smart's equations. These equations even lead to sediment transport rates q_s larger than the liquid flow discharge q for S_0 higher than 0.5, showing the limitations of such empirical formulations for steep slopes. On the contrary, the effect of the slope is more limited in the other formulations.

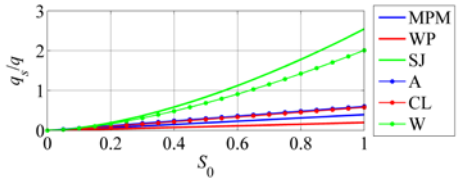

Figure 1 Sediment transport capacity for uniform flows with unit discharge q = 40 l/s/m

2.2 Impact of a stream-wise steep slope

There are two common ways to include the steep slope effect in the sediment transport: into the expression for the critical shear stress or into the expression for the effective shear stress. Fernandez-Luque and van Beek (1976, abbreviated FLvB) first deduced geometrically a correction factor for the critical shear stress on steep slopes:

$$\tau_{*c}(\alpha_0) = \tau_{*c0}\cos\alpha_0\left(1-\tan\alpha_0/\tan\varphi\right), \tag{1}$$

where τ_{*c0} is the critical shear stress on horizontal bed, α_0 is the local bed angle with respect to the horizontal (positive for a downsloping bed) and φ is the internal angle of friction of the bed material. This modification has however only few impact on sediment transport for dike overtopping test cases. Indeed, the effective shear stress ($\tau_* > 0.6$) is already far greater than the critical shear stress ($\tau_{*c} = 0.047$). So Wu (2004) proposed to add the streamwise component of the gravity force to the bed-shear stress, without changing the critical shear stress, so that the effective shear stress could be

$$\tau_*(\alpha_0) = \tau_{*0} + \lambda_0\tau_{*c0}\sin\alpha_0/\sin\varphi \tag{2}$$

where τ_{*0} is the shear stress on horizontal bed and λ_0 is an empirical coefficient:

$$\lambda_0 = \begin{cases} 1 & \alpha_0 \le 0 \\ 1+0.22\left(\tau_b'/\tau_c\right)^{0.15} e^{2\sin\alpha_0/\sin\varphi} & \alpha_0 > 0 \end{cases} \tag{3}$$

where the grain shear stress τ_b' is equal to the part of the shear stress not due to the bed-forms. This formulation was originally calibrated for Wu *et al.* (2000) sediment transport formulations.
If we compare the influence of both steep slopes modifications in sediment transport formulations (e.g. MPM formulation) we find the following expressions:

$$\begin{cases} \tau_* - \tau_{*c} = \tau_{*0} - f_{FLvB}\cdot\tau_{*c0} = \tau_{*0} - \tau_{*c0}\left[\cos\alpha_0\left(1-\tan\alpha_0/\tan\varphi\right)\right] \\ \tau_* - \tau_{*c} = \tau_{*0} - f_{Wu}\cdot\tau_{*c0} = \tau_{*0} - \tau_{*c0}\left[1-\lambda_0\sin\alpha_0/\sin\varphi\right] \end{cases} \tag{4}$$

So both formulations can be seen as a reduction of the critical Shields parameter. Figure 2 illustrates the comparison between the correction factor f_{FLVB} and the factor f_{Wu} with $\lambda_0 = 1$ and λ_0 calculated using Eq. (3). It can be seen that Wu and FLvB formulations are rather different for negative slopes (uphill). For positive slopes (downhill), the influence of the coefficient λ_0 is important, while FLvB and Wu formulations give similar correction factors if $\lambda_0 = 1$. Note that for these latter cases, $f = 0$ when $S_0 = \tan\varphi$, leading to a sediment transport for any value of τ_*, which is coherent for slopes steeper than the stability slope. However, for Wu formulation with λ_0 calculated following Eq. (3), we find $f = 0$ for slopes smaller than the stability slope, which is physically questionable.

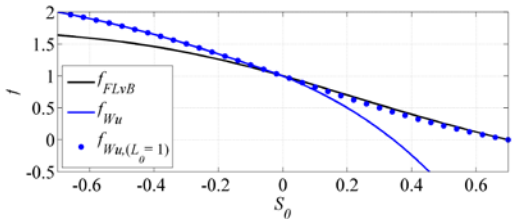

Figure 2 Slope factor correction: FLvB(dark line), Wu (blue line), and Wu with $\lambda_0 = 1$ (blue points)

2.3 Steep slope effect in Smart and Jäggi (1983) equation

Among the formulations presented in Table 1, Smart and Jäggi (1983) developed a bed-load transport equation especially designed for slopes up to 20%. First, the critical shear stress is adapted to account for the slope following Eq. (1). Moreover, the formulation of Smart and Jäggi (1983) depends directly on the energy slope S_f. This allows to account for the local slope in uniform flows for which $S_f = S_0$, but not in other cases. If S_f is replaced by the bed slope S_0, the sediment transport is set to zero on horizontal bed. So a modified formulation of Smart is proposed here, by replacing the energy slope S_f by the maximum between bed and energy slope $S = \max(S_0, S_f)$, leading to the following modified formulation:

$$q_{*s,MSJ} = 4.2\left(u/u_*\right)\max(S_0, S_f)^{\beta}\,\tau_*^{0.5}\left(\tau_* - \tau_{*c}(\alpha_0)\right) \tag{5}$$

3 NUMERICAL MODELS

One-dimensional clear water layer models assume one layer of pure water over a movable bed, while mixture layer models are based on direct exchange of sediment between the bed and the sediment-water mixture layer (Fig. 3). Both model are briefly described in the following sections, and then compared in section 3.3.

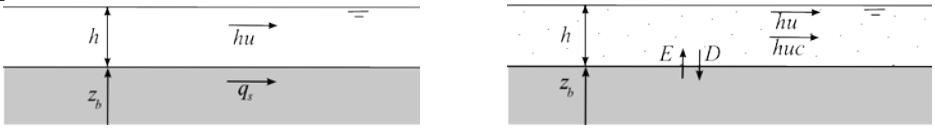

Figure 3 Clear-water layer (left) and mixture layer (right) models: idealized vertical flow structure

3.1 Clear water layer model

The equations of mass and momentum conservation of clear-water are coupled with a simplified Exner equation for sediment conservation, leading to the conservative vector form for a rectangular channel of unit width (Cunge and Perdreau 1973)

$$\frac{\partial \mathbf{U}}{\partial t} + \frac{\partial \mathbf{F}(\mathbf{U})}{\partial x} = \mathbf{S}_{CWL} \tag{6a}$$

where

$$\mathbf{U} = \begin{pmatrix} h \\ hu \\ z_b \end{pmatrix} \quad \mathbf{F} = \begin{pmatrix} hu \\ hu^2 + gh^2/2 \\ q_s/(1-\varepsilon_0) \end{pmatrix} \quad \mathbf{S}_{CWL} = \begin{pmatrix} 0 \\ g\,h\left(-\partial z_b/\partial x - S_f\right) \\ 0 \end{pmatrix} \tag{6b-d}$$

with h the flow depth, u the depth-averaged velocity, z_b the bed elevation, g the gravity acceleration, $-\partial z_b/\partial x$ the bed slope, S_f the friction slope based on Manning's formula, and ε_0 the bed porosity.

In this model, the actual sediment transport is considered to be equal to the local sediment transport capacity ($q_s = q_{scap}$), leading to what is usually referred to as an equilibrium sediment transport model. Using this simplification, and neglecting the sediment storage in the flow, the bed evolution can be directly linked to the sediment transport through the flux calculation. This system (Eq. 6) is solved in a coupled way using a first-order finite-volume scheme, with a standard splitting algorithm for the friction part of the source term $\mathbf{S}_{CWL}$ as

$$\begin{aligned}\mathbf{U}_i^p &= \mathbf{U}_i^n + \frac{\Delta t}{\Delta x}\left(\mathbf{F}_{i-1/2}^{*n} - \mathbf{F}_{i+1/2}^{*n}\right)\\ \mathbf{U}_i^{n+1} &= \mathbf{U}_i^p + \Delta t \mathbf{S}_{f,CWL}\left(\mathbf{U}_i^p\right)\end{aligned} \tag{7}$$

with n and n+1 the current and the next time step, and p indicating the intermediate state. The numerical fluxes across each cell interface in Eq. (7) are computed using the modified first-order Harten-Lax-Van Leer (HLL) scheme of Goutière *et al.* (2008). In this scheme, the wave speeds are estimated by means of approximate analytical expressions for the eigenvalues of the coupled system (Eq. 6). The bed slope source term is also treated in a lateralized way as suggested by Fraccarollo *et al.* (2003). Due to the explicit nature of the scheme, stability is dictated by the CFL condition on the time step Δt. Wetting and drying issues are treated by defining a threshold value of the water depth. If the flow depth in a cell is smaller than a prescribed value (typically 0.001 m), the cell is considered to be dry, and its velocity is set to zero.

3.2 Mixture layer model

The ML model considers mass and momentum equations for the mixture layer, and conservation equations for the sediment in the flow and in the bed (Cao *et al.* 2004, Wu and Wang 2008)

$$\frac{\partial \mathbf{V}}{\partial t} + \frac{\partial \mathbf{G}(\mathbf{V})}{\partial x} = \mathbf{S}_{ML} \tag{8a}$$

where

$$\mathbf{V} = \begin{pmatrix} h \\ hu \\ hc \end{pmatrix}, \mathbf{G} = \begin{pmatrix} hu \\ hu^2 + \dfrac{gh^2}{2} \\ huc \end{pmatrix}, \mathbf{S}_{ML} = \begin{pmatrix} (E-D)/(1-\varepsilon_0) \\ gh\left(-\dfrac{\partial z_b}{\partial x} - S_f\right) - \dfrac{(\rho_s-\rho_w)gh^2}{2\rho}\dfrac{\partial c}{\partial x} - \dfrac{(\rho_0-\rho)(E-D)u}{\rho(1-\varepsilon_0)} \\ E-D \end{pmatrix} \tag{8b-c}$$

$$\frac{\partial (z_b)}{\partial t} = \frac{D-E}{1-\varepsilon_0} \tag{9}$$

with c the depth-averaged sediment concentration in the water-sediment mixture, $\rho = \rho_w(1-c) + \rho_s c$ the depth-averaged mixture density, $\rho_0 = \rho_w \varepsilon_0 + \rho_s(1-\varepsilon_0)$ the density of saturated bed, E and D the sediment entrainment and deposition rates between the bottom and the flow layer, respectively. The net exchange of sediments is expressed as follows (Wu and Wang 2008):

$$D - E = \left(q_s - {q_s}^{cap}\right)/L \tag{10}$$

where $q_s = huc$ is the effective sediment transport rate per unit width, ${q_s}^{cap}$ is the equilibrium sediment transport rate, and L is the non-equilibrium adaptation length of sediment transport. For the test-case studied here, it has been observed that bed-load transport is predominant due to the use of sand. Therefore ${q_s}^{cap}$ is calculated using the bed-load formulations presented in Table 1 and $L = L_b$, the non-equilibrium adaptation length for bed-load. This parameter is usually taken as a calibrated coefficient, and is still subject to various uncertainties (Wu 2004).

As the bed deformation only depends on the erosion rate, Eq. (9) is solved separately. The three other equations form a hyperbolic system comparable to a classical hydrodynamic system with an advection equation. The effect of the sediment erosion / deposition is present through the source terms, and their role is therefore non negligible. The hyperbolic system (Eq. 8) can be solved in a coupled way using a first-order finite-volume scheme and a splitting algorithm for the source term as

$$\begin{aligned}&\mathbf{V}_i^p = \mathbf{V}_i^n + \frac{\Delta t}{\Delta x}\left(\mathbf{G}_{i-1/2}^{*n} - \mathbf{G}_{i+1/2}^{*n}\right)\\ &\begin{cases}\mathbf{V}_i^{n+1} = \mathbf{V}_i^p + \Delta t \mathbf{S}_{ML}(\mathbf{V}_i^p)\\ z_{b,i}^{n+1} = z_{b,i}^n + \Delta t\left((huc)_i^p - {q_s}^{cap}(\mathbf{V}_i^p)\right)/\left(L(1-\varepsilon_0)\right)\end{cases}\end{aligned} \tag{11}$$

The fluxes in Eq. (12) are computed using the HLLC (HLL with Contact discontinuities) scheme (Toro *et al.* 1994), modified to ensure the *C*-property of the system (Bermùdez and Vasquez 1994). For the second update of the cell states, the source terms are evaluated in each cell. The gradients of bed geometry and concentration in $\mathbf{S}_{ML}$ are solved by using a central-difference scheme. CFL stability condition and wetting-drying procedures are the same as for the CWL model.

4 EXPERIMENTAL DIKE MODEL

The models described previously are applied on an experimental dike overtopping test conducted at the Hydraulics Laboratory of the Université catholique de Louvain, Belgium (Van Emelen *et al.* submitted). As shown in Fig. 4, a sand dike was built in a 10-meter long, 0.2-meter wide and 0.3-meter high horizontal flume. The dike height is 0.20 m, the crest length 0.10 m, and the upstream and downstream slopes are 1V:2H. A 5-cm thick layer of sand is placed downstream of the dike, over a length of 1 m. The sand has a uniform size distribution with d_{50} = 0.61 mm.

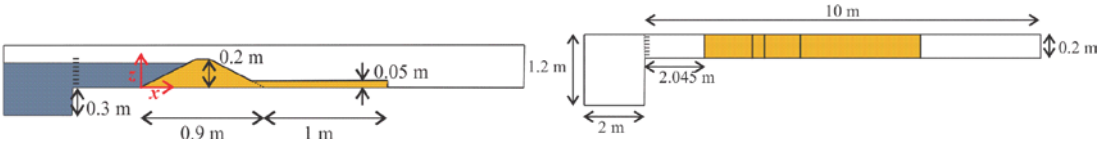

Figure 4 Flume and dike geometry: elevation (left) and plane view (right).

A 2-meter long and 1.2-meter wide storage reservoir is located upstream. This upstream reservoir is filled in with a constant inflow of 12 l/s. When the water level reaches 0.17 m, the inflow is set to zero, and then progressively re-increased at a constant rate of 0.25 l/s² until reaching the desired inflow. A constant inflow of 5 l/s (test 1) or 2.5 l/s (test 2) is maintained during all the duration of the overtopping test. Downstream of the flume, water and sand flow freely into a lower reservoir. Both the water-level and dike profiles were measured at various times. The initial time (t = 0 s) is determined when the upstream water level reaches the crest level (0.2 m). The overflow hydrograph was the theoretically calculated using a general overflow equation:

$$Q_b = C_d b\left(2gH_0{}^3\right)^{0.5} \tag{12}$$

with C_d the discharge coefficient, calculated using the formulation proposed by Schmocker et al. (2011), b the dike width, and H_0 the flow head upstream of the dike.

5 NUMERICAL RESULTS AND COMPARISON WITH EXPERIMENTAL DATA

5.1 Numerical model parameters

The sediment characteristics used for the numerical modeling are s = 2.65, ε_0 = 0.43, d_{50} = 0.61 mm, resulting in $n = d_{50}{}^{1/6}/21.1 = 0.0138$ s m$^{-1/3}$ following Strickler's (1923) formula. The mesh size Δx = 0.01 m and the CFL number is 0.9. The origin of the coordinate system (x, z) is taken at the upstream dike toe (Fig. 4). The boundary conditions include a free outflow downstream and an imposed hydrograph upstream of the reservoir, which is modeled with a length of 12 m and a width of 0.2 m to ensure the same storage capacity. For ML model, as the erosion is driven mainly by bed-load, the sediment transport can be considered as in nearly-equilibrium (Cao *et al.* 2012). So a short value of $L_b = \Delta x$ = 0.01 m has been chosen to avoid the formation of bed oscillations (Wu and Wang 2008).

5.2 Influence of the sediment transport formulation and steep slope correction

First of all, note that currently the ML model generates oscillations of the bed at dike crest and toe when using classical bed-load sediment transport formulations of Table 1. So the ML model is always used with the slope-corrected shear stress proposed by Wu *et al.* (2000) (Eq. 2) or with the modified formulation of Smart and Jäggi (2003) (Eq. 5). Indeed, it has been observed that the explicit account of the local slope ensures the stability of the model. Moreover, to ensure this stability of the bed, the slope

angle α_0 has to be calculated between the actual point and the bed level in the cell located immediately downstream. This oscillations problem is avoided with CWL model because this model already accounts for the local slope in the numerical solver for the sediment fluxes (Goutière *et al.* 2008).

This oscillation problem with the ML model has still to be solved, but the influence of the steep slope correction can already be analysed in the CWL model. Figure 5 compares dike profiles without slope correction, and with FLvB and Wu corrections. It can be seen that the influence of the steep slope correction is almost negligible on the dike profiles generated with the CWL model. This can be due to the account of the local bed levels in the numerical solver for the sediment fluxes (Goutière *et al.* 2008). This numerical account in the fluxes could be predominant in comparison with the correction proposed by FLvB or Wu.

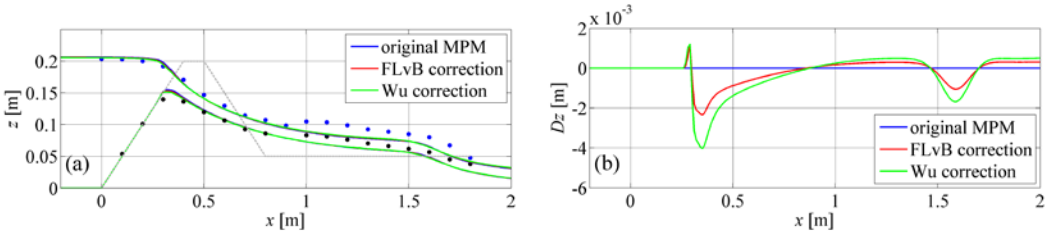

Figure 5 Influence of steep slope correction in sediment transport with CWL model and MPM formulation (test 2): dike profile at t = 24 s (a) and difference between original MPM and slope corrected formulations (b).

Figure 6 shows the dike profiles after 24 s and 64 s with the CWL model using various sediment transport equations for test 2. It can be seen that the formulation of Wong and Parker (2006) erodes clearly less than the other formulations. In the contrary, Abrahams (2003) formulation leads to an excessive erosion after 64 s. The other formulations give comparable results.

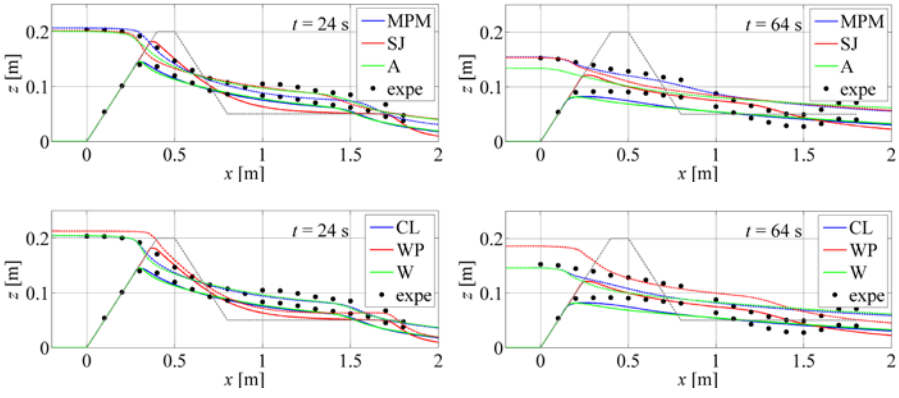

Figure 6 Comparison of dike profiles for test 2 at t = 24 s (left) and t = 64 s (right) with CWL model and various sediment transport equations.

5.3 Comparison of CWL and ML models

Figure 7 compares dike profiles for the CWL model with MPM formulation and the ML model with MPM sediment transport and Wu's correction for the slope. Although both models are based on distinct hypothesis, they lead to very similar results. Indeed, ML model is a little more complex by considering directly the impact of the sediment storage on the flow through a depth-averaged variable density. During the dike overtopping, the concentration reaches a maximum of c = 0.3 after 2 s, when the flow is very shallow on the downstream slope of the dike (h = 1.5 mm). Then the concentration falls to c = 0.16 at 12 s (h = 2.2 mm), c = 0.03 at 24 s (h = 18.8 mm) and c = 0.01 after 64 s (h = 28 mm). So the presence of sediment in the flow only plays a role during the first seconds of overtopping, while the model predicts an excessively small water depth. The second difference between both models is the inclusion of non-equilibrium sediment transport in the ML model. However, in case of pure bed-load transport, the adaptation length for sediment transport is rather small (Cao *et al.* 2012). This leads to a

nearly-equilibrium sediment transport, so both models give comparable results. The main difference in Fig. 7 is the slight rounding of the crest present in the CWL results at t = 24 s, which is still less important than the rounding observed in the experimental results.

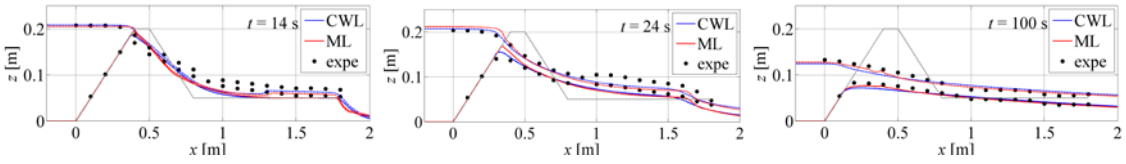

Figure 7 Dike profiles at t = 14 s, 24 s and 100 s for test 2 and test 1: CWL model with original MPM formulations and ML model with MPM sediment transport and Wu's correction for the slope.

Globally, it can be seen in Fig. 7 that both models predict quite well the dike profiles and upstream water level at various times. However, the simulated water depth during the first seconds of erosion is too small, and deposition at the downstream dike toe after 14 s is not high enough. Moreover, the numerical models do not simulate the antidunes observed experimentally (also seen in Fig. 6 at t = 64 s).

The crest elevation and shape has also a big impact on the overflow discharge, which is the most important parameter in real situations to evaluate the flood downstream of the dike. Figure 9a presents the outflow hydrograph computed with the CWL model for test1, while Fig. 9b compares the root mean square error of the peak outflow in comparison with the peak outflow deduced from the experimental data, for both numerical models and both tests.

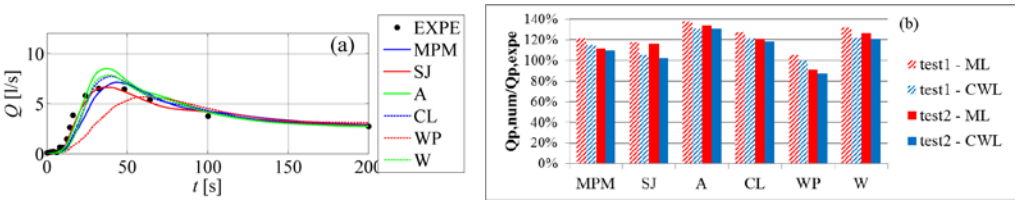

Figure 8 Outflow hydrographs for test 2 with CWL model (a) and numerical peak discharge in comparison with experimental peak discharge for both models and both tests (b)

As WP formulation erodes too slowly, the consecutive overflow hydrograph is temporally delayed (Fig. 9a) and the peak outflow is slightly underestimated, especially for test 2 (Fig. 9b). On the contrary, Abrahams formulation gives the higher peak outflow for both tests with both numerical models. The four other formulations give comparable outflow hydrographs for test 2 with the CWL model. Among them, SJ and MPM formulations give the more accurate peak outflow, with RMSE between 100 and 120%

6 CONCLUSIONS

This paper presents a study on sediment transport modelling over steep slopes, with a particular focus on simulating the erosion of an earthen dike by overtopping. Several empirical sediment transport formulations are selected and compared. However, as those formulae were developed for flows over moderate bed slopes, two correction factors are studied to account for the impact of a steep slope on the sediment transport estimation. The first correction is proposed by Fernandez-Luque and van Beek (1976) and is applied on the critical shear stress. The second correction, proposed by Wu (2004), modifies the effective sediment transport. It is shown that both formulations give different results, with Wu's formulation predicting infinite sediment transport for slopes lower than the stability slope. Two numerical models are implemented and tested using the selected sediment transport formulations: the first one is based on the Clear Water Layer (CWL) assumption, while the second one is a Mixture Layer (ML) model. Both sets of equations are solved using a first order finite volume scheme, with HLL and HLLC solvers for the fluxes. These two models are applied on a dike overtopping experimental test-case, representing a small-scale sand dike with a sand layer downstream of the dike. The numerical results are compared to the experimental measurements, with a special attention on the impact of the sediment transport formulation, of the steep slope correction factor, and of the choice of the numerical model.

It is shown that the steep slope correction factors in the sediment transport equations have a very limited impact on the results produced by the CWL model. However, these correction factors are essential with the ML model. Indeed, it has been observed that the explicit account of the local slope ensures the stability of the model, while the model generates oscillations of the bed when used with classical sediment transport formulations. The various sediment transport formulations are then compared with the CWL model. It is shown that Wong and Parker (2006) equation clearly underestimates the erosion while Abrahams (2003) formulation lead to an excessive erosion. The other formulations give comparable results. With the same sediment transport equation, ML model and CWL model also give comparable results, provided that Wu's slope correction factor is used with the ML model. This is partly due to the use of a very small adaptation length in the non-equilibrium sediment transport formulation of the ML model. The results are then close to the results obtained by the equilibrium sediment transport in the CWL model. Finally, the outflow hydrographs and the peak outflow are compared for each sediment transport formulation and each model. Again Wong and Parker (2006) and Abrahams (2003) show the more discrepancies with the experimental data, for CWL and ML model. Meyer-Peter and Müller (1948) and Smart and Jäggi (1983) formulations give the more accurate results. Further research will be carried out especially to improve the stability of the ML model and to study the effect of the slope correction factor on this model. Finally, a two-dimensional extension will be investigated, with a special focus on finding an expression for the slope correction factor adapted to two dimensional problems.

References

Abrahams, A. (2003). Bed-Load Transport Equation for Sheet Flow. *J. Hydraul. Eng*., 129(2), 159–163.

Bermùdez, A., and Vázquez, M. E. (1994). Upwind methods for hyper-bolic conservation laws with source terms. *Comput. Fluids*, 23(8),1049–1071.

Camenen, B. and Larson, M. (2005). A general formula for non-cohesive bed load sediment transport. *Estuarine Coastal Shelf Sci.*, 63(1–2), 249–260.

Cao, Z., Pender, G., Wallis, S., Carling, P. A. (2004). Computational dam-break hydraulics over erodible sediment bed. *J. Hydraul. Eng*., 130(7), 689–703.

Cao, Z., Li, Z., Pender, G., and Hu, P. (2012) Non-capacity or capacity model for fluvial sediment transport. *Water management ICE*, 165(4), 193-211.

Capart, H., and Young, D. L. (1998). Formation of a jump by the dam-break wave over a granular bed. *J. Fluid Mech.*, 372, 165–187.

Cunge, J. A., and Perdreau, N. (1973). Mobile bed fluvial mathematical models. *Houille Blanche*, 28(7), 561–580

El Kadi Abderrezzak, K. and Paquier, A. (2011). Applicability of sediment transport capacity formulas to dam-break flows over movable beds. *J. Hydraul. Eng*., 137(2), 209-221.

Fernandez Luque, R., and van Beek, R. (1976). Erosion and transport of bed-load sediment. *J. Hydraul. Res.*, 14(2), 127-144.

Fraccarollo, L., Capart, H., Zech, Y. (2003). A Godunov method for the computation of erosional shallow water transient. *Intl. J. Numer. Meth. Fluids*, 41, 951–976.

Goutière, L., Soares-Frazão, S., Savary, C., Laraichi, T., Zech, Y. (2008). One-dimensional model for transient flows involving bedload sediment transport and changes in flow regimes. *J. Hydraul. Eng*., 134(6), 726–735.

Greco, M., Iervolino, M., Vacca, A., and Leopardi, A. (2012) Two-phase modelling of total sediment load in fast geomorphic transients. *Proc. Int. Conf. on Fluvial Hydraul. - River Flow 2012* (1), San Jose, Costa Rica, 643-648

Meyer-Peter, E. and Müller, R. (1948). Formulas for bed load transport. *Proc., 2nd Meeting, IAHR*, Stockholm, Sweden, 39–64.

Schmocker, L., Halldórsdóttir, B.R., Hager, W.H. (2011). Effect of weir face angles on circular-crested weir flow. *J. Hydraulic Eng*., 137(6), 637-643

Smart, G. M., and Jäggi, M. N. R. (1983). Sediment transport on steep slopes. Mitteilungen der Versuchsanstalt für Wasserbau, Hydrologie und Glaziologie, Vol. 64, Eidgenössische Technische Hochschule (ETH), Zürich, Switzerland

Strickler, A. (1923). Beitraege zur Frage der Geschwindigkeits-formel und der Rauhigkeitszahlen für Ströme, Kanäle und geschlossene Leitungen. Mitteilung 16. Eidgenössisches Amt für Wasserwirtschaft, Bern, Switzerland (in German).

Toro, E. F., Spruce, M., and Speares, W. (1994). Restoration of the Contact Surface in the HLL-Riemann Solver. *Shock Waves*, 4, 25–34.

Van Emelen, S., Ferbus, V., Spitaels, T., Zech, Y., and Soares-Frazão, S. Experimental investigation of the erosion of a sand dike by overtopping. Submitted to the 2013 IAHR congress, Chengdu, China.

Wong, M., Parker, G. (2006). Reanalysis and correction of bed-load relation of Meyer-Peter and Müller using their own da-tabase. *J. Hydraul. Eng*., 132(11), 1161–1168.

Wu, W., Wang, S.S.Y., Jia, Y. (2000). Nonuniform sediment transport in alluvial rivers. *J. Hydraul. Res*., 38(6),

427-434
Wu, W. (2004). Depth-averaged two-dimensional numerical modeling of unsteady flow and non-uniform sediment transport in open channels. *J. Hydraul. Eng.*, 130(10), 1013-1024.
Wu, W. and Wang, S.S.Y. (2008). One-dimensional explicit finite-volume model for sediment transport with transient flows over movable beds. *J. Hydraul. Res*., 46(1), 87–98.
Zech, Y., Soares-Frazão, S., Spinewine, B., Le Grelle, N. (2008). Dam-break induced sediment movement: Experimental approaches and numerical modelling. *J. Hydraul. Res*., 46(2), 176–190.